Applied Physics A (2020) 126:456
https://doi.org/10.1007/s00339-020-03621-3

Applied Physics A
Materials Science & Processing

Magnetic field and temperature-dependent studies of structural and magnetic properties of $NiFe_2O_4$ films

Kanchan Kumari[1] · Rajesh Kumar[1] · Partha Bir Barman[1]

Received: 4 April 2020 / Accepted: 11 May 2020 / Published online: 26 May 2020

Abstract
Unheated and heated nickel ferrite ($NiFe_2O_4$) films under the influence of the magnetic field were fabricated using a solution method named as the liquid–vapor interfacial method. The effect of magnetic field and temperature on the morphological, structural, and magnetic properties of the films was studied. The particle size is found to increase from both SEM images and XRD calculations. From the XRD calculations, the particle size in unheated films increases from 7.3 to 18.9 nm, and in heated films, from 22.3 to 24.9 nm with the application of a magnetic field. The interplanar spacing and lattice constant increase with the applied magnetic field and decreased with heating. From the XPS results, the atomic percentage of cation at tetrahedral and octahedral sites shows the mixed spinel structure of formed ferrite films. All the magnetic factors are found to increase by implementing the magnetic field while decrease with the heating of films.

1 Introduction

Spinel ferrite thin films are attracting interest because of their different magnetic properties, which include ferromagnetism, ferrimagnetism, and antiferromagnetism. This spinel structure permits the incorporation of different metallic ions to change their properties [1, 2]. These materials show high magnetic permeability, electric resistivity, significant magnetostrictive coefficients, and saturation magnetization. They have utility in several areas such as in the enhancement of the information storage area, in the technology of ferrofluids, wave industries, disk-recording magnetic refrigeration, transducer devices, multilayer chip inductors, and as gas sensors [2–5]. $NiFe_2O_4$ is one of the important members of the spinel ferrite group, which is a soft magnetic material having an inverse spinel structure and ferrimagnetic properties. The structure of ferrite can be understood from the distribution of divalent and trivalent ions in tetrahedral voids and octahedral voids. For the inverse spinel structure, $x = 1$, where x is an inversion factor defined as a number of trivalent ions occupy tetrahedral sites [6, 7]. The ferrimagnetic nature of the $NiFe_2O_4$ appears due to the arrangement of magnetic moments of the spins of Fe^{3+} ions at tetrahedral sites and that of Ni^{2+}, Fe^{3+} ions at octahedral sites [2, 3, 6, 8]. $NiFe_2O_4$ films are suitable for device applications from lower millimeter to upper microwave wave ranges [4].

Thin films are the most suitable nanostructure for many applications because of their different properties from the bulk. The microstructure of thin film is an important parameter in determining their magnetic properties, which can be affected by varying the growth methods and growth parameters [9]. The growth methods for spinel ferrite thin films include sol–gel [10], spin spray plating [11], magnetron sputtering [12, 13], pulsed-laser deposition [14], etc. The growth parameters include temperature, lattice mismatch, deposition time, thin-film strain, surface morphology, microstructure, and chemical composition [1, 9]. The heating temperature affects the properties of ferrites by varying their cation distribution and the grain size. The heating temperature affects the microstructure of films, and hence, a change in the properties can be seen.

As far as we know, there are only limited number of reports available for the comparative studies of unheated and heated $NiFe_2O_4$ films, and no report is available for the unheated and heated $NiFe_2O_4$ films formed in the presence of a magnetic field. In this study, we have prepared Ni-ferrite films without and with the application of the external magnetic field applied during their growth and then again made two sets, one is unheated and the other is heated at a low temperature (300 °C). Then, the effect of temperature,

✉ Rajesh Kumar
rajesh.kumar@juit.ac.in

[1] Department of Physics and Materials Science, Jaypee University of Information Technology, Waknaghat, Solan, Himachal Pradesh 173234, India

along with the magnetic field on the properties of $NiFe_2O_4$ films, is studied.

2 2 Experimental procedure

The liquid–vapor technique is used for the formation of films reported in this work. The starting materials were polyvinyl alcohol (PVA), nickel chloride ($NiCl_2$), and ferric chloride ($FeCl_3$) salts, which are used to make precursor solution. For making the precursor solution, 0.4 g of PVA is dissolved in 100 ml of distilled water, and after that, hexahydrated $CoCl_2$ and $FeCl_3$ salts were added in proper stoichiometric proportions to the PVA solution. To obtain a clear solution, the solution was stirred for 20 min at 40 °C using a hot plate magnetic stirrer. The finally prepared solution was then allowed to cool down and filtered. For the preparation of films, the precursor solution was taken into the petri dish and placed inside a closed chamber. Thereafter, magnetic field of 1 T was applied to the precursor solution and a measured amount of NH_3 vapors was purged inside the chamber. A time of 15 min was given for the reaction of NH_3 vapors with the precursor solution. After the reaction of 15 min, the petri dish was taken out of the chamber; a floating film formed on the surface of the solution was then transferred to the surface of a glass substrate. To study the effect of temperature on the formed films, a set of films was kept unheated, and the other set was heated at 300 °C in a furnace for 1 h in an argon environment. Also, to study the effect of a magnetic field along with the temperature, the films were also formed without and with the application of in-plane orientation of the magnetic field.

3 Result and discussion

3.1 Scanning electron microscopy

The scanning electron micrographs (SEMs) of unheated and heated $NiFe_2O_4$ films prepared without and with the magnetic field are shown in Fig. 1. All the micrographs show a smooth and uniform morphology. Although from the SEM images, there seems no apparent difference in the particle size of the unheated films prepared without (Fig. 1a) and with (Fig. 1b) magnetic field. However, a significant difference is obtained in the corresponding histograms, which are estimated from a Image J software. The average particle size estimated for the unheated films prepared without and with the magnetic field is 9.3 and 20.6 nm, respectively. These films, when heated at 300 °C, demonstrated a further increase in the particle size, as shown in Fig. 1c, d. The average particle size now increased to 27.9 to 29.2 nm, respectively. Thus, both the applied magnetic field and the heating conditions influence the average particle size in the films.

3.2 X-ray Diffraction

X-ray diffraction pattern of the $NiFe_2O_4$ films prepared without and with the magnetic field, and before and after heating is shown in Fig. 2. The peak in all the patterns corresponding to the films reveals spinel structure of $NiFe_2O_4$. According to the standard JCPDS card (74-1913), the peaks are indexed as a cubic $NiFe_2O_4$ phase. Using the broadening of (220) peak in XRD pattern, the particle size has been calculated with the help of Scherrer's equation $D = \frac{k\lambda}{\beta \cos\theta}$ where λ is wavelength, β is difference of full width at half maximum and instrumental broadening, and θ is Bragg's angle.

The calculated crystallite size for unheated samples prepared without and with the magnetic field is 7.3 nm and 18.9 nm, while for the heated samples, it increases to 22.3 nm and 24.9 nm, respectively. The interplanar spacing and lattice constant for unheated samples prepared without and with the magnetic field increase from 2.84 to 2.86 Å and 8.03 to 8.09; for the heated samples, they increase from 2.80 to 2.82 Å and 7.92 to 7.98, respectively. Both the interplanar spacing and lattice constant are found to decrease with the heating of films prepared without and with the magnetic field. The decrease in the crystal lattice parameters, for heated samples, can be attributed to the extermination of point defects due to the thermal vibrations, as reported in [15–17]. Nonetheless, the films were heated in an oxygen-deficient argon environment that may also result in the depletion of oxygen ions/atoms inside the film, which therefore causes a decrease in the lattice constant as observed.

The distortion of the lattice was estimated by calculating dislocation density and vacancy defects. The dislocation density (δ) is calculated using the relation $\delta = \frac{1}{D^2}$ with crystallite size (D). Also, the concentration (β) of cation/anion vacancy is calculated by using $\beta = \frac{\left(a_{th}^3 - a_{exp}^3\right)}{a_{th}^3} \times 100\%$, where a_{th} is the theoretical lattice constant from JCPDS card (74-1913), and a_{exp} is experimentally calculated lattice constant [18]. For the unheated samples prepared without and with the magnetic field, the value of δ is 18.7 $m^2 \times 10^{15}$ and 2.79 $m^2 \times 10^{15}$, respectively. Upon heating the films, the value of δ reduces to 2.01 $m^2 \times 10^{15}$ and 1.61 $m^2 \times 10^{15}$, respectively. The variation is also estimated by calculating the coefficient of structural deformation (ε) from the relation $\varepsilon = \frac{a_{th} - a_{exp}}{a_{th}}$, where a_{th} and a_{exp} are the theoretically and experimentally calculated lattice constants, respectively [19]. The calculated value of ε for unheated films prepared without and with the magnetic field is 0.0276 and 0.0203, which upon heating changes to 0.0409 and 0.0336, respectively. Next, the value of β for

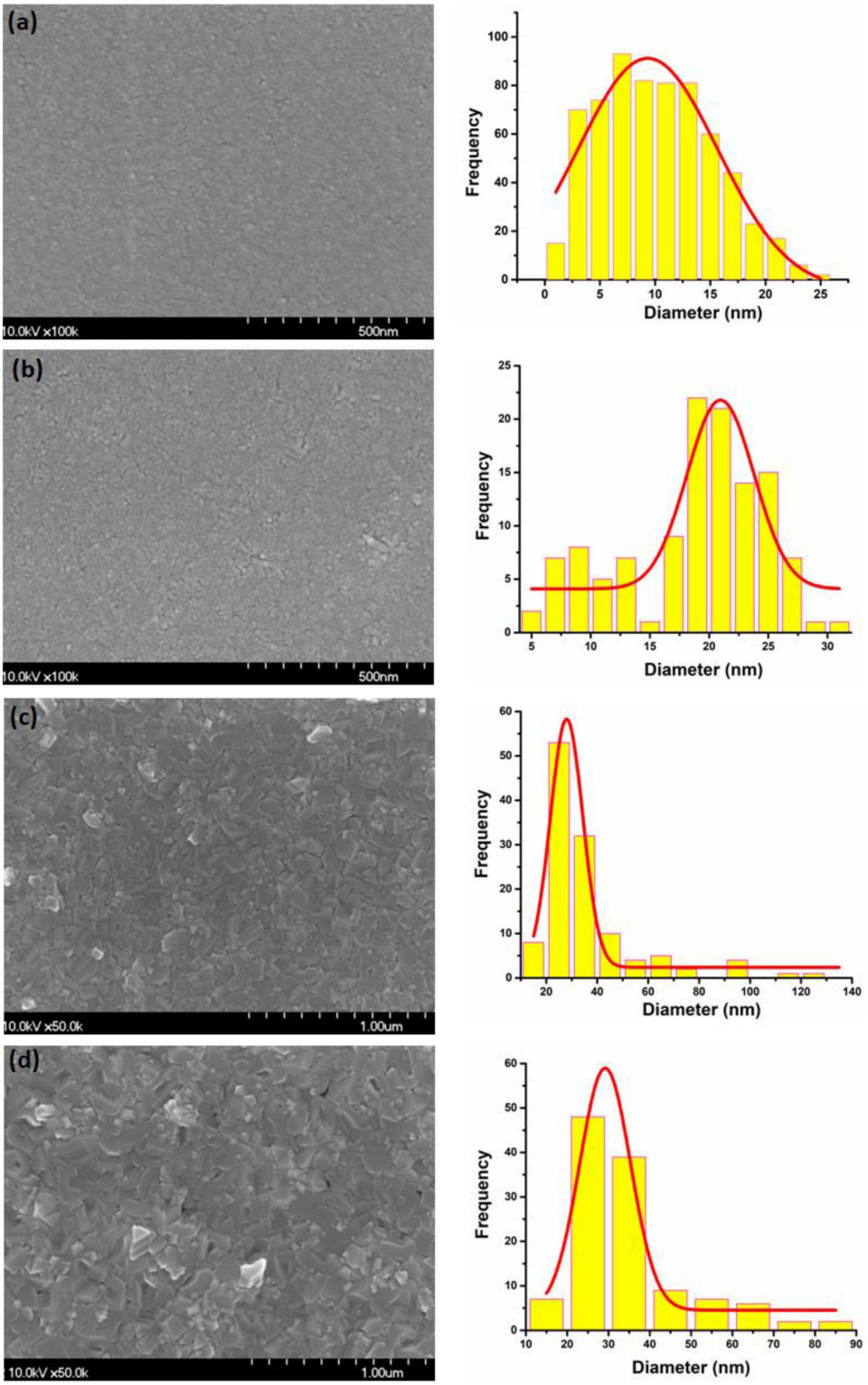

Fig. 1 SEM images of $NiFe_2O_4$ films along with particle size distribution; **a** unheated and **c** heated film prepared without a magnetic field, **b** unheated, and **d** heated film prepared by the implementation of an in-plane magnetic field

the unheated samples prepared without and with the magnetic field is 8.07 and 5.97%, and upon heating, it increases to 11.78 and 9.76%, respectively. The observed variations in the values of δ and β indicate lattice distortions/dislocation in the films due to the implementation of the magnetic field and heating.

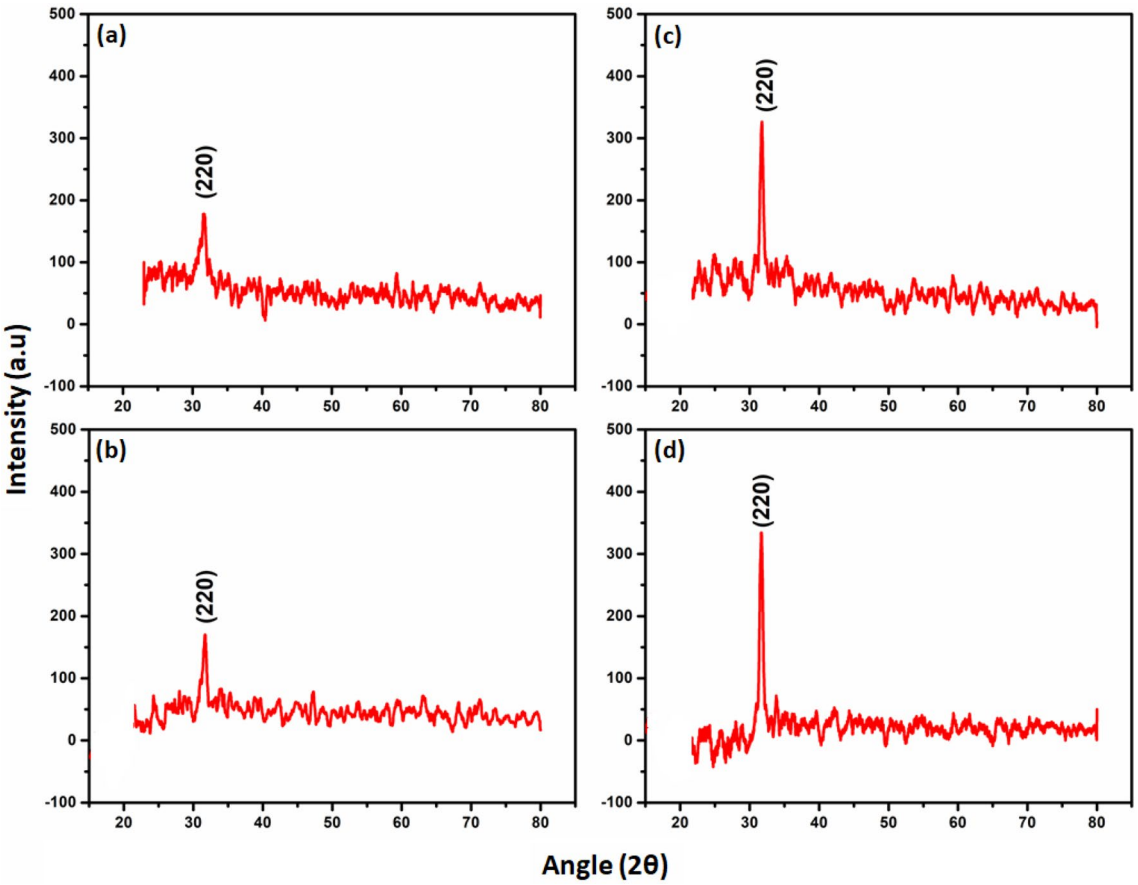

Fig. 2 X-ray diffraction pattern of $NiFe_2O_4$ films; **a** unheated and **c** heated film prepared without a magnetic field, **b** unheated and **d** heated film prepared by the implementation of an in-plane magnetic field

3.3 X-ray photoelectron spectroscopy

The survey spectra of $NiFe_2O_4$ films are shown in Fig. 3. Figure 3a, e shows survey spectra of unheated and heated films of $NiFe_2O_4$ films formed without applying the magnetic field during film formation. Distinct peaks of O1s, Fe2*p*, and Ni2*p* are observed in both survey spectrums, while the carbon peak may come as a contamination from the air, or organic component remained in the samples or is just an instrumental impurity. A high-resolution spectrum of Fe2*p*, Ni2*p*, and O1*s* signals was also collected and is shown in Fig. 3b–d for unheated films and Fig. 3f–h.

Figure 3 shows the high-resolution spectra of Fe2*p* corresponding to the unheated (Fig. 3b) and heated (Fig. 3f) $NiFe_2O_4$ ferrite films. Octahedral and tetrahedral occupancy of Fe in $NiFe_2O_4$ is observed by the deconvolution of the spectra. The two peaks (Fig. 3b) at the positions 724.5 eV and 710.7 eV of binding energy correspond to Fe2$p_{1/2}$ and Fe2$p_{3/2}$, respectively. From the satellite features of Fe2*p*, the oxidation state of Fe cation is revealed 3+. The Fe2$p_{3/2}$ peak is then deconvoluted, which has two components with binding energies of 710.7 eV and 713.4 eV; these correspond to the Fe cations at octahedral and tetrahedral sites, respectively. The atomic percentages of Fe^{3+} cation in octahedral and tetrahedral sites are estimated quantitatively from peak area calculations, which are found to be 79.0 and 21.0%, respectively. For the heated films (Fig. 3f), the deconvoluted peaks of Fe2$p_{3/2}$ are found at 710.4 and 713.2, and the atomic percentage at octahedral and tetrahedral sites is found to be 78.9% and 21.1%, respectively.

For Ni2*p*, the unheated film (Fig. 3c) has Ni2$p_{1/2}$ peak at the binding energy 873.84 eV and that of the peak Ni2$p_{3/2}$ at 855.59 eV. The peak Ni2$p_{3/2}$ is further deconvoluted to represent the occupancy of Ni in octahedral and tetrahedral sites and has two components at 855.9 eV and 857.8 eV. The atomic percentage from peak area calculations is calculated as 86.4 and 13.6% for the octahedral and tetrahedral sites, respectively. The satellite feature reveals the 2+ oxidation state of nickel. For the heated films (Fig. 3g), the deconvoluted Ni2*p* spectra show two components at 854.7 eV and 856.4 eV, which shows the occupancy of Ni^{2+} cations in octahedral and tetrahedral sites. Here the atomic percentage is found to be 73.6% and 26.4%, respectively.

From the XPS results, it is found that the percentage of Fe^{3+} cations remains almost the same, whereas Ni^{2+} cations

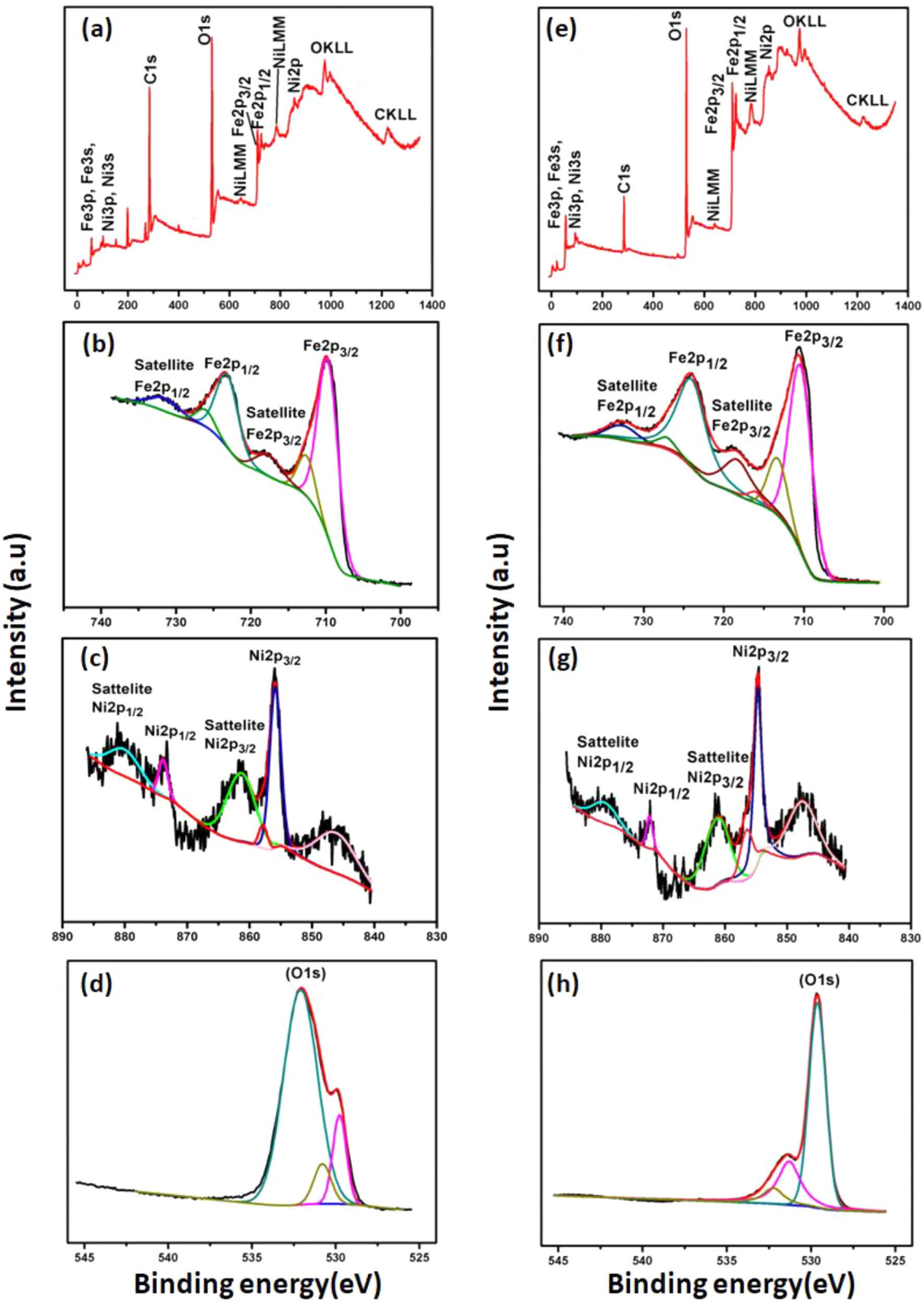

Fig. 3 XPS spectrum for $NiFe_2O_4$ films. **a** and **e** represent the survey spectrum, **b** and **f** represent high-resolution Fe2*p* spectrum, **c** and **g** represent high-resolution Ni2*p* spectrum, and **d** and **h** represent high-resolution O1*s* spectrum for unheated and heated samples, respectively

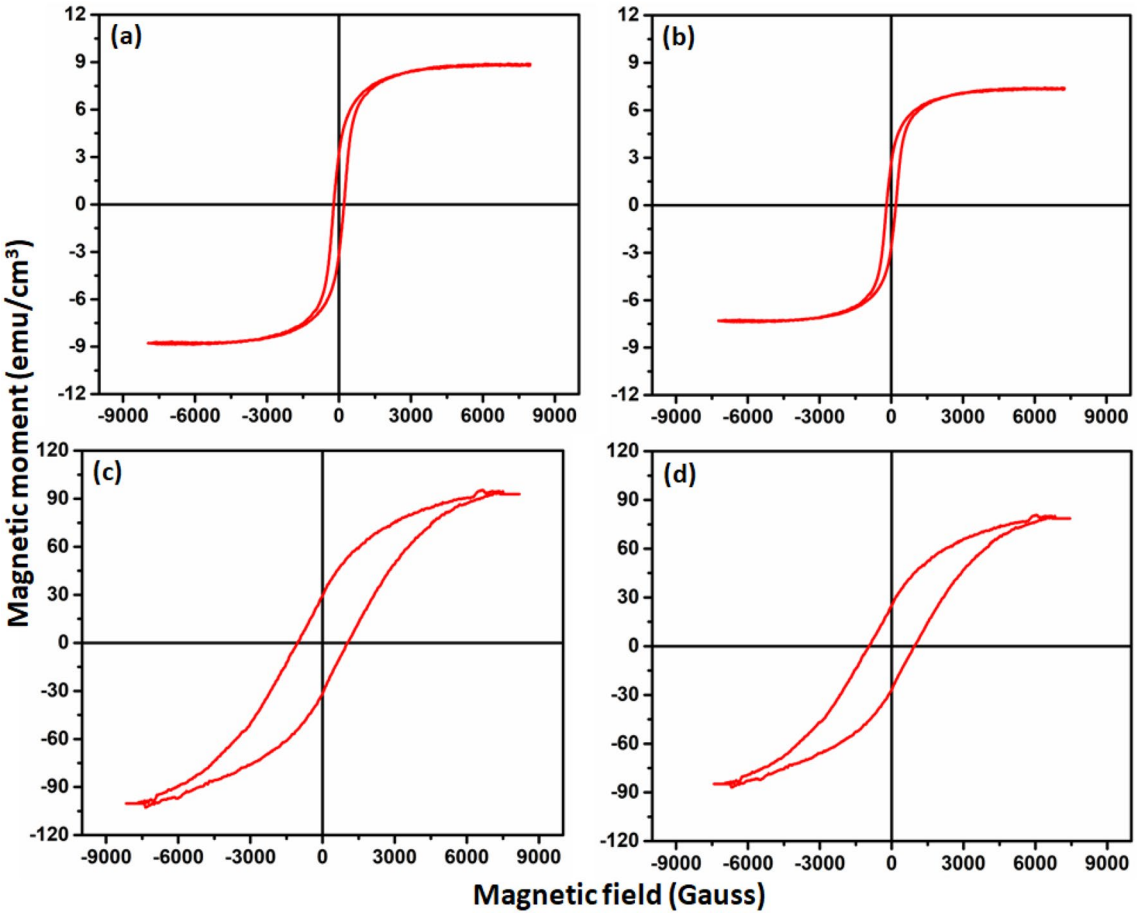

Fig. 4 Hysteresis and magnetic properties variation for $NiFe_2O_4$ films; **a** unheated and **c** heated film prepared without the magnetic field, **b** unheated, and **d** heated film prepared by applying an in-plane magnetic field

show variation at the tetrahedral and octahedral sites, as it decreases at octahedral and increases at tetrahedral sites. Generally, to occupy the tetrahedral site, cations push oxygen ions along the body diagonals of an inverse spinel structure, and result in a shrinking of tetrahedral sites that produce a strain [20]. However, in a case where the formation temperature is sufficiently high, the strain is reduced by occupying the octahedral sites rather than tetrahedral sites. In our case, the XPS results show that only the tetrahedral occupancy increases after heating the films that indicates an insufficient formation temperature to what is required for diverting the Ni^{2+} cations toward octahedral sites. Therefore, the observed increasing tetrahedral occupancy of the Ni^{2+} cations is expected to shrink the overall crystalline structure, and thus a reduction in the lattice parameters as observed from the XRD results.

Figure 3 shows high-resolution O1s spectra for unheated (Fig. 3d) and heated (Fig. 3h) $NiFe_2O_4$ films, respectively. The unheated film formed without magnetic field, has the highest peak at 532.1 eV, second-highest peak at 529.6 eV and third peak at 531.1 eV. Similarly, the heated film, the highest peak is found at 529.6 eV, second-highest peak is at 531.3 eV and the third peak at 532.2 eV. The peak at 529.6 eV corresponds to lattice oxygen (O^{2-}) as at this point, spinel 3D metal gets oxidize. The peak at 532.2 eV corresponds to structural defects, such as under-coordinated lattice oxygen and chemisorbed oxygen, and the peak at 531.3 eV is just the result of fitting asymmetry of the XPS peak. In the unheated sample, the peak with binding energy 532.1 eV dominates, whereas in the heated sample the peak with the binding energy 529.6 eV dominates. This is because in unheated sample, there may be the formation of OH^- ions and after heating these ions are removed, and only the lattice oxygen is left. The decrease in the intensity of peak at 532.2 eV indicates the decrease in the structural defects after heating, which also affects the lattice parameters.

3.4 Vibrating sample magnetometer

The room temperature hysteresis measurement for unheated and heated films prepared with and without magnetic field $NiFe_2O_4$ films is shown in Fig. 4. The magnetic parameters

such as saturation magnetization, coercivity, retentivity, and anisotropy of the films and their variation with the applied magnetic field and with heating were calculated from the hysteresis loop. For the unheated film prepared without a magnetic field (Fig. 4a), the saturation magnetization, coercivity, and retentivity values are found 8.78 emu/cm^3, 215.23 Oe, and 3.15 emu/cm^3, respectively. While for the heated film formed without magnetic field (Fig. 4b), the value of saturation magnetization, coercivity, and retentivity decreased to 7.33 emu/cm^3, 195.78 Oe, and 2.68 emu/cm^3, respectively. The value of magnetic factors for unheated films prepared in the presence of the magnetic field (Fig. 4c) is 96.74 emu/cm^3, 1028.27 Oe, and 30.87 emu/cm^3 for saturation magnetization, coercivity, and retentivity, respectively. For the heated films formed with magnetic field, the magnetic factors, saturation magnetization, coercivity, and retentivity values decreased to 81.69 emu/cm^3, 950.75 Oe, and 26.15 emu/cm^3, respectively. It can be seen that with the heating of films, all the magnetic factors decrease. This may be due to the different cation distributions at octahedral and tetrahedral sites. The magnetic properties of $NiFe_2O_4$ arise from the magnetic moments of Fe^{3+} ions located in tetrahedral voids and Ni^{2+}, Fe^{3+} located at octahedral voids [2, 3, 6, 8]. From the XPS results, we can clearly see that the atomic percentage of Ni^{2+} and Fe^{3+} decreases with the heating of films and hence results in the decrease in overall remained magnetic moment and hence the magnetic factors.

4 Conclusion

Heated and unheated films of $NiFe_2O_4$ formed without and with magnetic fields are successfully formed on the surface of a glass substrate. SEM images and XRD calculations clearly show that the particle size increases with the heating of films, and also with the application of magnetic field. Whereas, the interplanar spacing and lattice constant are found to be increase with the applied magnetic field, and decrease with the heating of the films. The XPS results show that the formed hydroxides are successfully converted to oxides after heating. The atomic percentage of cations at octahedral and tetrahedral sites shows the mixed spinel structure of the formed ferrite films, which is influenced by the heating of the films. All the magnetic factors are found to increase with the application of the magnetic field, whereas they decrease with the heating of the films.

Acknowledgements This work is supported by the research grant of CVD Laboratory, Department of Physics and Materials Science, Jaypee University of Information Technology, Waknaghat, Solan, India.

References

1. N. Li, S. Schäfer, R. Datta, T. Mewes, T.M. Klein, A. Gupta, Appl. Phys. Lett. **101**, 2010 (2012)
2. Y. Köseoğlu, M. Bay, M. Tan, A. Baykal, H. Sözeri, R. Topkaya, N. Akdoğan, J. Nanoparticle Res. **13**, 2235 (2011)
3. F.L. Zabotto, A.J. Gualdi, J.A. Eiras, Mater. Res. **15**, 428 (2012)
4. A.R. Chavan, R.R. Chilwar, P.B. Kharat, K.M. Jadhav, J. Supercond. Nov. Magn. **31**, 2949 (2018)
5. M. Penchal Reddy, W. Madhuri, M. Venkata Ramana, N. Ramamanohar Reddy, K.V. Siva Kumar, V.R.K. Murthy, K. Siva Kumar, R. Ramakrishna Reddy, J. Magn. Magn. Mater. **322**, 2819 (2010)
6. P.B. Koli, K.H. Kapadnis, U.G. Deshpande, J. Nanostructure Chem. **9**, 95 (2019)
7. K. Maaz, A. Mumtaz, S.K. Hasanain, M.F. Bertino, J. Magn. Magn. Mater. **322**, 2199 (2010)
8. P. Chavan, L.R. Naik, Phys. Status Solidi Appl. Mater. Sci. **214**, 1 (2017)
9. G. Dixit, J.P. Singh, R.C. Srivastava, H.M. Agrawal, R.J. Chaudhary, Adv. Mater. Lett. **3**, 21 (2012)
10. P. Gao, E.V. Rebrov, T.M.W.G.M. Verhoeven, J.C. Schouten, R. Kleismit, G. Kozlowski, J. Cetnar, Z. Turgut, G. Subramanyam, J. Appl. Phys. **107**, 044317–18 (2010)
11. C.M. Fu, H.S. Hsu, Y.C. Chao, N. Matsushita, M. Abe, J. Appl. Phys. **93**, 7127 (2003)
12. M. Desai, S. Prasad, N. Venkataramani, I. Samajdar, A.K. Nigam, N. Keller, R. Krishnan, E.M. Baggio-Saitovitch, B.R. Pujada, A. Rossi, J. Appl. Phys. **91**, 7592 (2002)
13. L.Z. Li, Z. Yu, Z.W. Lan, K. Sun, R. Di Guo, J. Magn. Magn. Mater. **368**, 8 (2014)
14. C.N. Chinnasamy, S.D. Yoon, A. Yang, A. Baraskar, C. Vittoria, V.G. Harris, J. Appl. Phys. **101**, 2005 (2007)
15. A.L. Kozlovskiy, I.E. Kenzhina, M.V Zdorovets, Ceram. Int. **46**, 10262 (2020)
16. K. Egizbek, A.L. Kozlovskiy, K. Ludzik, M.V. Zdorovets, I.V. Korolkov, Ceram. Int. **46**, 16548 (2020)
17. M. V Zdorovets, A. L. Kozlovskiy, Sci. Rep. **9**, 16646 (2019)
18. A.L. Kozlovskiy, I.E. Kenzhina, M.V. Zdorovets, M. Saiymova, D.I. Tishkevich, Ceram. Int. **45**, 17236 (2019)
19. M.V Zdorovets, A.L. Kozlovskiy, J. Mater. Sci. Mater. Electron. **29**, 3621 (2017)
20. Z. Cvejic, E. Durdic, G.Ivkovic Ivandekic, B. Bajac, P. Postolache, L. Mitoseriu, S.R. Srdic, J. Alloys Compd. **649**, 1231 (2015)